



**SPE 131297**

## **Effect of gas type on foam film permeability and its implications for foam flow in porous media**

R. Farajzadeh, SPE, Shell International E&P, R.M. Muruganathan, Max-Planck Institute of Colloids and Interfaces (MPI), Germany, R. Krastev, NMI Natural and Medical Sciences Institute at the University of Tuebingen, Germany, W.R. Rossen, SPE, Delft University of Technology, The Netherlands

Copyright 2010, Society of Petroleum Engineers

This paper was prepared for presentation at the SPE EUROPEC/EAGE Annual Conference and Exhibition held in Barcelona, Spain, 14–17 June 2010.

This paper was selected for presentation by an SPE program committee following review of information contained in an abstract submitted by the author(s). Contents of the paper have not been reviewed by the Society of Petroleum Engineers and are subject to correction by the author(s). The material does not necessarily reflect any position of the Society of Petroleum Engineers, its officers, or members. Electronic reproduction, distribution, or storage of any part of this paper without the written consent of the Society of Petroleum Engineers is prohibited. Permission to reproduce in print is restricted to an abstract of not more than 300 words; illustrations may not be copied. The abstract must contain conspicuous acknowledgment of SPE copyright.

---

### **Abstract**

The ability of foam to control the gas mobility in porous media is determined in part by the trapped (stationary) fraction of foam,  $X_t$ . The common approach to determining  $X_t$  is to replace some part of the gas by a “*tracer gas*” during the steady-state stage of the experiments and fitting the effluent data to a capacitance mass-transfer model. Diffusion between bubbles is quantified by the film permeability coefficient,  $K$  (cm/s). We measured the film permeability coefficient of different gases for foam films made of four surfactants. The results show that the value of  $K$  is largely dependent on the dissolution of gas in the surfactant solution and increases with increasing gas solubility in the bulk liquid. The measured values of  $K$  are consistent with rapid diffusion of tracer through trapped gas adjacent to flowing gas in porous media, and difficulties in interpreting the results of tracer-foam experiments with conventional capacitance models. Effective diffusion coefficients of gases through trapped foam can be estimated from  $K$ . These diffusion coefficients differ substantially, and this implies swelling or shrinkage of trapped gas from diffusion. The implications of the results for foam flow in porous media is discussed in detail and some suggestions are given to improve the measurements and modeling of trapped fraction of foam.

### **1. Introduction**

Foam is a dispersion of a gas phase in a continuous liquid phase stabilized by surfactants and/or nano-particles (Exerowa and Kruglyakov, 1998; Binks and Horozv, 2005). In the petroleum industry, to prevent early breakthrough of gas (typically steam, CO<sub>2</sub>, N<sub>2</sub> or enriched hydrocarbons) into the production wells, gas can be injected together with a surfactant solution into the geological formation. In this way, and under certain circumstances, viscous foam forms and controls gas mobility. Foam in porous media is made up of gas bubbles that are separated by thin liquid films, i.e., lamellae, which span across pores. Foam efficiency in reducing the gas mobility, to a large extent, depends on its trapped fraction, i.e., the fraction of foam that does not flow and remains stationary even as a high-pressure gradient is applied (Fried, 1961; Kovscek and Radke, 1994; Rossen, 1996). When the pressure gradient is not high enough to keep a given lamella moving, the lamella becomes trapped in the pore throat and gas flow is blocked. Experimental measurements reveal that the fraction of the gas that is not flowing during foam flow can be as high as 0.99 or greater (Tang and Kovscek, 2006; Radke and Gillis, 1990; Kil et al., 2009). In the trapped fraction of foam, unless lamellae break, gas transport system is limited by slow diffusion through the foam films (Cohen et al, 1996, 1997).

Initially the lamellae between foam bubbles are thick, but due to the capillary pressure in the meniscus water drains out of the lamellae and they become thinner. Finally, equilibrium films are obtained with a uniform thickness depending on the concentration

of the ions in the solution. There are two equilibrium states of foam films that are defined by thermodynamic conditions. *Common films* are usually formed when the salt concentration in the film-forming solution is low and the electrostatic double layer repulsion between the film surfaces is strong. These films have a sandwich-like structure (Figure 1) and consist of two monolayers of adsorbed surfactant molecules separated by an aqueous layer. The film thickness decreases as the salt concentration in the film-forming solution increases. The reflectivity from the film decreases so much at a certain film thickness (and corresponding salt concentration) that the film looks black in reflected light. Therefore these films are called *Common Black Films* (CBF). Their stability, according to the classical DLVO approach (Deryaguin and Landau, 1941; Verwey and Overbeek, 1948) is due to the interplay between the repulsive electrostatic ( $\Pi_{EL}$ ) and the attractive van der Waals ( $\Pi_{v,w}$ ) components of the disjoining pressure,  $\Pi$ .  $\Pi_{EL}$  decreases with the further addition of salt to the film-forming solution until it is fully suppressed. Very thin *Newton Black Films* (NBF) are formed at that point. These films have bilayer structures: the two surfactant monolayers are close to each other, separated only by few layers of hydration water. The stability of these films is governed by the interplay of the short-range interaction forces. The application of DLVO theory to such thin foam films is limited because the theory does not take into account both spatial and/or surfactant density fluctuations (Israelachvili and Wennerstrom, 1992). To our knowledge, there is no direct experimental evidence on the type (and equilibrium thickness) of the films formed in a porous medium.

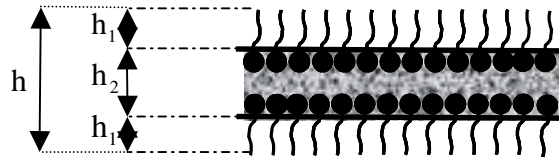


**Figure 1:** A single foam film consists of an aqueous core with thickness  $h_2$  sandwiched between two adsorbed monolayers of surfactant with the thickness of  $h_1$ . The liquid and monolayers are assumed to be homogenous.

The purpose of this paper is to investigate the effect of gas type on the gas permeability of foam films stabilized by different types of surfactant. Our focus is on the implication of the results for foam flow in porous media and the accuracy of the techniques used for measuring the trapped fraction of foam. The structure of the paper is as follows: First we provide the relations for film permeability and discuss the interpretations of tracer experiments. The details of the experimental technique and materials are explained in Section 2. Section 3 presents the experimental results for different gases and discusses the possible explanations for the observations. Section 4 gives insight into the application of these results in interpreting the tracer gas experiments and determining the trapped fraction of foam. Finally we draw the main conclusions of this study.

### 1.1. Foam film permeability

A measure of the gas permeability of a foam film is the permeability coefficient  $K$  (m/s) (Brown et al, 1953; Princen and Mason, 1965; Barnes, 1986) defined by

$$J = \frac{dn}{dt} = -KS\Delta C_g \quad (1)$$

where  $J$  is rate of transport of gas through the film (mole/s),  $n$  is the number of moles of gas (mol),  $t$  is time (s),  $S$  is the area of the film ( $\text{cm}^2$ ), and  $\Delta C_g$  is the concentration difference of the gas on both sides of the film ( $\text{mole}/\text{cm}^3$ ). Considering the film structure in Figure 1, a detailed expression for the permeability was proposed by Princen and Mason (1965):

$$K = \frac{D_w H}{h_2 + 2D_w / k_{ml}} \quad (2)$$

Here  $D_w$  is the diffusion coefficient of the gas in the aqueous core of the film ( $\text{cm}^2/\text{s}$ ),  $H$  is the dimensionless Henry's-law constant for the solubility of the gas in the aqueous solution (-),  $k_{ml}$  is the permeability coefficient of a single surfactant monolayer ( $\text{cm}/\text{s}$ ) and  $h_2$  is the film aqueous core thickness (Figure 1) (cm). For sufficiently thick films,  $h_2 \gg 2D_w / k_{ml}$ , the permeability is characterized by the transport properties of the gas through the aqueous core. The film permeability increases with decreasing film thickness whereas the thickness of the monolayers remains constant. If  $h_2 < 2D_w / k_{ml}$  the gas permeability is governed by the permeability of the adsorbed monolayers  $k_{ml}$ . Different mechanisms for the permeation through surfactant monolayers and their advantages in explaining foam film permeability are proposed in the literature (Farajzadeh et al, 2008a; Barnes et al, 1983).

Princen and Mason (1965) derived the following relation for the permeation rate of a multi-component gas,  $K_G$ :

$$K_G = \left( \sum_{i=1}^n \frac{x_i}{K_i} \right)^{-1} \quad (3)$$

where  $n$  is the number of components and  $x_i$  and  $K_i$  are the mole fraction and permeability of the film to component  $i$ , respectively. Essentially this equation implies that the diffusion process of a multi-component gas through foam films is similar to a pure gas and that gases diffuse independent of each other. Princen and Mason (1965) argue that the gases diffuse out from the bubble nearly in the same ratio as their respective mole fractions in the bubble, so that the mole fractions subsequently change very slowly.

## 1.2. Tracer experiments to determine trapped-gas fraction in foam

The rate of diffusion of tracer through lamellae plays a key role in interpretation of tracer experiments to determine the trapped-gas fraction in foam in porous media. In an ideal coreflood tracer experiment, once steady-state foam flow is established, the paths of flowing gas do not change, and foam advances down all flow paths at the same velocity. If there is no dispersion along the flow path and no diffusion into the surrounding trapped gas, the tracer breakthrough time in the effluent is directly proportional to the flowing-gas fraction of the foam. In practice, however, tracer enters the trapped gas by diffusing through lamellae separating the flowing- and trapped-gas bubbles, and analysis is more complicated.

In the capacitance model of Radke and Gillis (1990), an effective mass-transfer coefficient between flowing and trapped gas accounts for the lamella surface area between them and mass-transfer through these lamellae. One fits the effluent tracer concentration over time to a capacitance model for convection and mass transfer and infers the flowing-gas fraction from this fit. As mass-transfer rate increases, it becomes harder and harder to infer the trapped-gas fraction from the effluent profile. In the limit of very fast mass transfer, the effluent profile is indistinguishable from that of convection-dispersion with no trapped gas (Kil et al., 2009).

Kil et al. present a method of inferring flowing-gas fraction from CT images of Xe tracer distribution in a foam-tracer experiment. In this approach, it is crucial to estimate the effective diffusion coefficient of tracer through trapped foam in advance. Li et al. (2010), using the geometry shown in Figure 2, present a simple model relating the film-permeability coefficient  $K$  to the effective diffusion coefficient  $D_e$  ( $\text{cm}^2/\text{s}$ ) for tracer through the trapped foam over distances much larger than a single bubble:

$$D_e = \frac{KSL^2}{V} \quad (4)$$

where  $S$  is area of a lamella in a pore throat ( $\text{cm}^2$ ) and  $L$  is the distance between lamellae in the direction of diffusion (cm). For diffusion through bubbles in a cylindrical tube,  $D_e = KL$ .

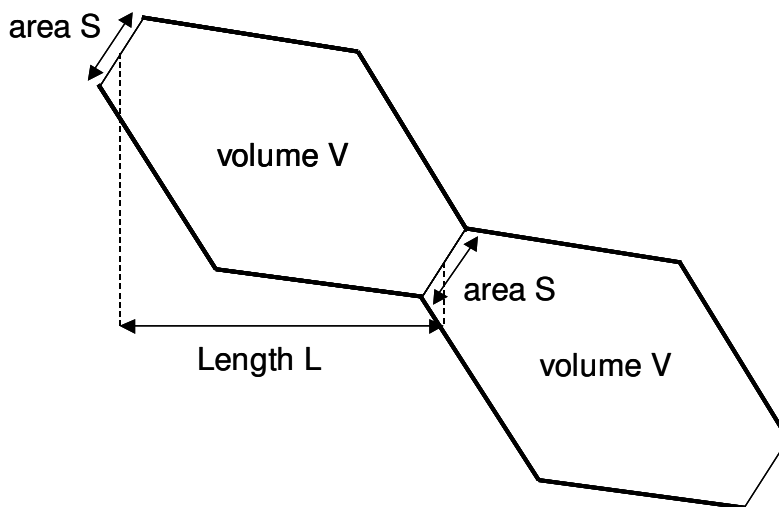


**Figure 2:** Model for derivation of effective diffusion coefficient of foam in a porous medium, represented as a periodically constricted tube. Lamellae occupy the pore throats. Gradient of tracer concentration is in horizontal direction, and lamellae are a distance  $L$  apart in this direction. Bubbles have volume  $V$ , and lamellae area  $S$ .

In equimolar counter-diffusion through stagnant, ideal gases, a mole-centered reference frame does not move during the process. For diffusion of tracer  $A$  through a porous medium filled with trapped foam made with gas  $B$ , both  $A$  and  $B$  diffuse through lamellae that do not move. The permeabilities of  $A$  and  $B$  through lamellae can be quite different, as shown below. Consider the implications in a simple case where the diffusion coefficient of  $A$  through films is much greater than that of  $B$ .  $A$  begins to diffuse from flowing gas through lamellae into trapped-gas bubbles full of gas  $B$  long before  $B$  begins to diffuse in the opposite direction. Ultimately, diffusion responds to chemical potential, which for ideal gases is proportional to partial pressure. Thus as  $A$  diffuses into the trapped bubbles and their total pressures rise, the driving force for diffusion of  $A$  (low partial pressure of  $A$  inside the bubbles) remains. In principle, the rise in pressure in the trapped gas could be great. For instance, if back-pressure is 40 bar (Alvarez et al., 2001) and mole fraction of  $A$  in flowing gas is 25% as in Nguyen et al. (2009), then diffusion of  $A$  into the trapped gas would continue until the partial pressure in the trapped gas is 10 bar, and total pressure in the trapped gas is 50 bar, 10 bar higher than the pressure in the flowing gas. Two tracers, each at 10% mole fraction, were used simultaneously in the study of Tang and Kovscek (2006), with 8 bar back-pressure and an inlet pressure of about 23 bar, which suggests a potential rise in pressure of about 5 bar in the trapped gas near the inlet. In Nguyen et al.'s experiment, upstream pressure was 6 bar, so the pressure in the trapped gas could rise 1.5 bar. As pressure begins to rise, however, trapped-gas bubbles would expand into the flowing-gas pathways and be carried downstream with the flowing gas (or possibly break). In this way the interpretation of the experiments is made more complex.

If gas  $B$  diffuses through foam lamellae much faster than tracer  $A$ , the trapped gas would shrink as it loses component  $B$  to the flowing gas. When lamellae separating trapped gas from flowing gas had withdrawn substantially back from their pore throats, new lamellae would be deposited by the moving bubbles in these pore throats by lamella division (Rossen, 1996). Again, interpretation of the experiment is made more complex.

If one gas (say,  $B$ ) diffuses through lamellae much more slowly than the other, it could accumulate at high concentration in the gas near the lamella surface, slowing the transport of  $A$  to the lamella. This is the principle behind addition of non-condensable gas to steam foam (Falls et al., 1988), where transport of steam across lamellae (not by diffusion, but by condensation and evaporation) is much faster than diffusion of nitrogen across the same lamellae. In that case transport of steam across the lamella is controlled by heat conduction through the lamella, which is orders of magnitude faster than diffusion (Bird et al., 2002); there is so little resistance to heat transfer in the lamella that diffusion of steam through the gas near the lamella controls the process. In a tracer experiment, where two gases diffuse to the surface and then through the lamella, however, the main resistance is transport through the lamella, not diffusion through the gas. Diffusion coefficients in gases are orders of magnitude greater than those through liquid, especially when liquid surface is covered by surfactant monolayer (Farajzadeh et al, 2008a; Janssen and Warmoeskerken, 2006). Therefore, diffusion through the gas is not a significant factor in rate of transport between bubbles. We believe that two or more gases would diffuse virtually independently of each other; the slower-diffusing component would not slow down transport of the others, in agreement with Princen and Mason (1965).

## 2. Experimental section

### 2.1. Experiment: Permeability through a single foam film

Film permeability was measured using the "*diminishing bubble*" method described earlier in detail (Nedyalkov et al, 1992; Krustev et al, 1996). The experimental setup is shown in Figure 3. The studied solution is placed in a small Teflon vessel with a diameter of 1 cm. The small radius of the vessel allows the solution to form a convex surface after it is introduced. The solution and the space above it are saturated with the desired gas to make sure that the gas diffuses through the film and not into the liquid. A small floating bubble with radius  $R_b$  of about 100  $\mu\text{m}$  is formed under the solution/gas interface. The bubble floats to the surface, and a foam film with radius  $r$  is formed on its top. Because of the curvature of the surface, the bubble is fixed in its centre. It is observed from below through the glass bottom of the Teflon vessel in reflected light. The film formed on the top of the bubble is observed simultaneously in transmitted light with a second microscope. Both microscopes equipped with video cameras are coaxial. This allows simultaneous observation and video analysis of the radius of the bubble and the radius of the film. The small bubble radius insures that the bubbles keep their spherical shape, and they are not affected by gravity (Platikanov et al., 1980; Dimitrov, 1977). A schematic of the bubble floating on the liquid surface and the forces that act on it is shown on Figure 4.

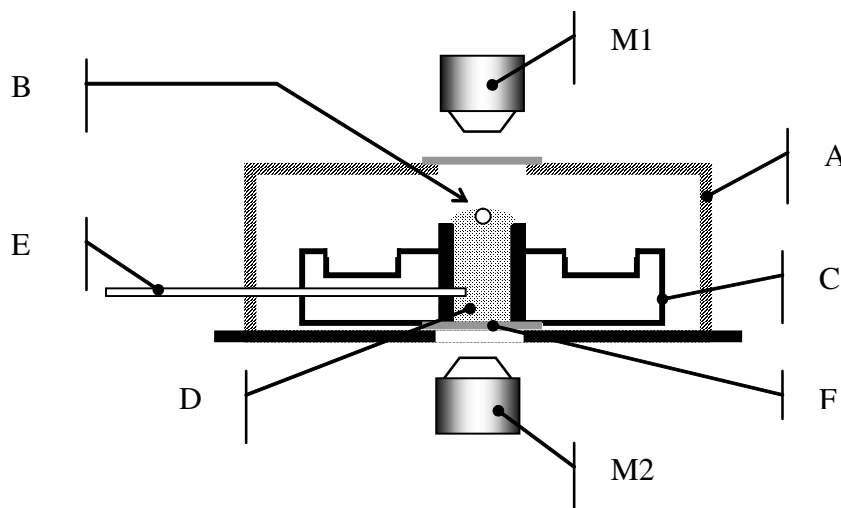


**Figure 3:** Schematic of the experimental cell: (A) brass box, (B) bubble, (C) Teflon vessel, (D) aqueous solution, (E) syringe for bubble formation, (F) glass window, (M1) and (M2) microscopes

The gas pressure in the bubble is higher than atmospheric pressure  $P_{at}$  in the space above the solution because of capillary pressure  $P_c$ . The capillary pressure varies during the experiment, typically from 700 Pa to 1000 Pa. This overpressure is the driving force for the permeation of gas through the thin foam film formed at the top of the bubble. The capillary pressure in the bubble may be expressed either by the film tension  $\gamma$  and the radius of the curvature of the film  $R_f$  (not shown on the Figure) or by the surface tension  $\sigma$  at the gas/solution interface and the radius of the bubble  $R_b$ . The experimental setup allows  $R_b$  to be easily measured.  $\sigma$  is measured separately. Thus, the difference in the gas concentrations inside and outside the bubble is given by:

$$\Delta C_g = \frac{P_c}{R_A T} = \frac{2\sigma}{R_b R_A T} \quad (5)$$

Here,  $R_A$  is the universal gas constant and  $T$  is the temperature. As a consequence of permeation, the bubble shrinks, and  $R_b$  and  $r$  decrease with time. Since the gas is treated as ideal, the number of moles of the gas in the bubble  $n(t)$  decreases with time  $t$  according to:

$$n(t) = \left( P_{at} + \frac{2\sigma}{R_b(t)} \right) \frac{4}{3} \pi R_b^3(t) / R_A T \quad (6)$$

If the film on the top of the bubble is approximated with a circle with radius  $r$  instead of a spherical cap, the area of the film (i.e. the area through which the permeability occurs) is:

$$S(t) = \pi r^2(t) \quad (7)$$

This last approximation introduces an error of less than 3% of the calculation of the film area for films with areas much smaller than the area of the bubble (Krustev et al., 1996). The extended exact formula for calculating the permeability, which takes into account the precise shape of the foam film on top of a free-floating bubble, is given elsewhere (Nedyalkov et al., 1988). Using Eq. (6) and integration over time yield the following relation for calculation of  $K$  from the experimentally obtained time dependencies of the film and bubble radii

$$K = \left[ (P_{at}/2\sigma)(R_{b0}^4 - R_{bt}^4) + \frac{8}{9}(R_0^3 - R_t^3) \right] \left( \int_0^t r^2 dt \right)^{-1} \quad (8)$$

Here,  $R_{b0}$  and  $R_{bt}$  are respectively the values of  $R$  at the beginning ( $t = 0$ ) and at the end ( $t = t$ ) of the experiment. The numerical evaluation of Eq. (8) is performed using a calculating procedure described by Krustev et al. (1996). The precision of the method is  $\pm 0.002$  cm/s. The experiments were performed at constant-temperature, controlled with a precision of  $\pm 0.1$  °C. All presented  $K$  values are arithmetical mean values from more than 5 individual experiments. The standard deviation of the mean values are presented as error bars in the figures. All experiments with different gases were performed at surfactant concentrations above the critical micelle concentration (cmc) at the respected conditions (salt concentration, temperature).

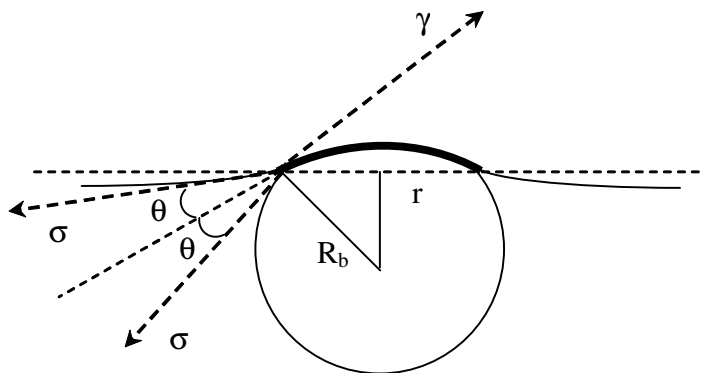


**Figure 4:** Schematic of a small freely floating bubble at the gas/aqueous solution interface and the foam film formed on top of it:  $\sigma$  is surface tension between solution and gas;  $\gamma$  film tension,  $\theta$  contact angle between film and meniscus;  $R_b$  radius of the bubble and  $r$  radius of the film.

### 3.2. Materials

**Surfactants:** Four surfactants were used to make foam films. (1) Sodium dodecyl sulfate (SDS), (2) Dodecyl tri-methyl ammonium bromide (C12TAB), (3) Dodecyl  $\beta$ -maltoside (C12G2), and (4) (C<sub>14</sub>-C<sub>16</sub>)-alpha-olefin sulfonate (AOS). The details of surfactants are presented in Table 1.

Sodium chloride (NaCl) GR grade (Merck, Darmstadt, Germany) was roasted at 600°C for 5 hours to remove surface-active contaminants. All solutions were prepared with water of Milli-Q quality (Elga Labwater, Germany). The specific resistance of the water was better than 18.2 M $\Omega$ cm, the pH was 5.5 and the total organic carbon (TOC) value was less than 10 ppb. All solutions were exposed to sonication (SONOREX RK52, Bandelin, Berlin, Germany) before the experiments.

All gases, except air, were with purity 5 and delivered from Air Liquide, Berlin, Germany. The gases were saturated to water vapor before the experiments. Thus the evaporation from the solutions was reduced and the stability of the studied films was increased.

**Table 1:** List of surfactants used in the experiments

Name	Name	Type	$\sigma$ (mN/m), at c.m.c.	Provider
SDS	Sodium dodecyl sulfate	anionic	25	Henkel, Germany. Specially purified at MPI to remove C <sub>12</sub> OH contaminations.
C <sub>12</sub> TAB	Dodecyl tri-methyl ammonium bromide	cationic	25	Sigma-Aldrich
$\beta$ -C <sub>12</sub> G <sub>2</sub>	$\beta$ -dodecyl maltoside	nonionic	34	Luckenwalde, Germany
AOS	Alpha olefin sulfonate	anionic	24	Stepan, USA

### 3. Results and discussion

The permeabilities (diffusion rates) of films prepared from different surfactant solutions were determined for four gases, namely Argon (Ar), Oxygen (O<sub>2</sub>), Nitrogen (N<sub>2</sub>), Air (A) and in one case, Xenon (Xe). An attempt was made to measure the permeability of films to CO<sub>2</sub>; however, the shrinkage was so fast that it was not possible to quantify the permeation rate of CO<sub>2</sub>. The reported permeabilities are the average values of at least five single measurements.

For each surfactant the measurements were done for two electrolyte concentrations. For ionic surfactants, at lower NaCl concentrations CBFs are formed, which typically have equilibrium thickness of about 10-15 nm. At higher NaCl concentrations NBFs with approximate thickness of 5 nm are formed (Muruganathan et al. 2004; Farajzadeh et al., 2008b). For  $\beta$ -C<sub>12</sub>G<sub>2</sub> because of the weak charge of interfaces the barrier for the transition from CBF to NBF is very low and therefore only NBFs are formed under our experimental conditions (Muruganathan et al., 2004).

One can estimate the importance of the surfactant monolayer using Eq. (2) and calculating  $K$  assuming that the monolayers play no part in film permeability. If film permeability depends solely on diffusion through the water layer,  $K=DH/h_2$ . For nitrogen

taking values of  $D$  and  $H$  from Table 3, for a film thickness of 26 nm, one estimates  $K$  to be about 0.1 cm/s, which is comparable to the measured value of  $K$ . However, for the thickness of 15 nm one calculates  $K$  of about 0.18 cm/s that is higher than actual value of  $K$ . This suggests that as film surfaces approach each other, and in the range that surfaces forces become important, the monolayer becomes a dominant part of the overall transport through the films. In other words, surfactants adsorbed on film surfaces can hinder the transfer rate of gases by about one order of magnitude, even though their effect on transfer through films thicker than 20-30 nm and through a gas-liquid interface in bulk solutions (Hanwight et al., 2005) is not significant. For NBFs and CBFs we cannot calculate effective diffusion coefficients as interaction between film surfaces also play important role on their permeability.

One would expect higher permeation rate for thinner films; however, as it can be seen from Figure 5 for the anionic surfactant, and for all gases (compare gas permeabilities of NBFs and CBFs in Figure 6 with those in Figure 7), CBFs have larger permeability than NBFs. It has been previously reported that the permeability of films stabilized by SDS (Krustev et al, 1993; Krustev and Müller, 1999) and AOS (Farajzadeh et al, 2009a), both to air, slightly increases when the film thickness decreases from its initial value (about 50 nm) down to a thickness of 15 nm, where CBFs start to form. The gas permeability of the films is governed in this range of thicknesses by the permeability of the central aqueous layer of the film. After that point (peak in the permeability vs. thickness or salt concentration plot) the gas permeability decreases most probably because the film permeability is governed by the monolayer permeability, and consequently the adsorption density of the surfactant monolayers. A decrease of the film permeability of the thinnest foam film NBF was already reported for other systems. This behavior depends on the type of surfactants. For example it is not observed for non-ionic or cationic surfactants. It looks to be a characteristic for foam films in which the contact angle between the film and the meniscus is large. The decrease of the  $K$  after the maximum value can be explained by reduced permeability of the monolayers. This might be a result of increased adsorption upon increase of the electrolyte concentration. Note that adsorption of surfactant molecules on foam films might be different than on bulk surfaces.

Based on free energy of film formation Krustev and Müller (1999) has given an alternative explanation for this behavior. According to their theory when (as a result of increase of salt concentration) the absolute value of free energy of film formation increases the adsorption of surfactant molecules on film surface also increases and thus gas permeability of films decreases. Moreover, the monolayer permeability, which governs the permeability through very thin films, depends on the area in the monolayers accessible for gas molecules to pass through. This area can be described by the number of unoccupied sites in the adsorption layer. At the transition to the NBF, this number and therefore the accessible areas decreases due to the effect of the film interaction on the state of the monolayers.

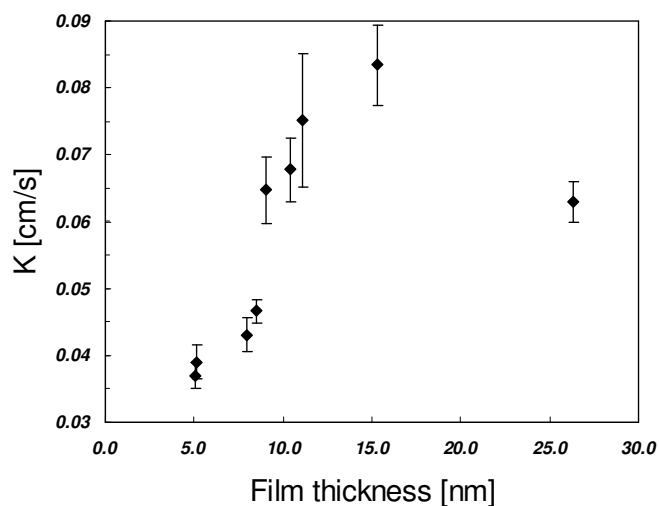


**Figure 5:** Air permeability of foam films stabilized by AOS as a function of the film thickness (data taken from Farajzadeh et al., 2009).

Another interesting feature of the experiments is the considerable effect of type of the surfactant on permeability of the gases. First, the gas permeabilities of CBFs and NBFs for non-ionic and cationic surfactants are similar and  $K$  is insensitive to film thickness. Second, compared to anionic surfactants, the films made by the non-ionic surfactant have much lower permeabilities while the films made by the cationic surfactant have larger permeabilities. This conclusion is valid for all gases. This means that for nonionic surfactant, the adsorption on the film surface is higher because of the lack of charge in the surfactant molecules. Thus, the molecules are better packed staying very close to each other at the film surface. For cationic surfactants the positive charge of

molecules induces larger repulsive forces, which keeps them apart. Therefore, the available area for permeation of gas is larger in cationic surfactants leading to higher permeability coefficients.

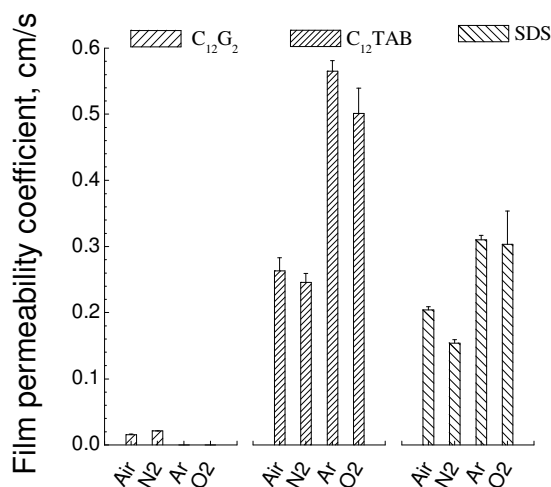


**Figure 6:** Gas permeability of CBF stabilized by  $\beta$ -C<sub>12</sub>G<sub>2</sub>, C<sub>12</sub>TAB, SDS to different gases.

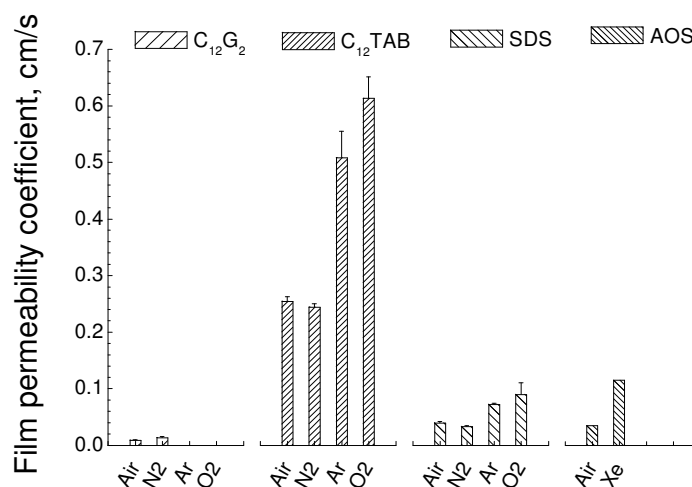


**Figure 7:** Gas permeability of NBF stabilized by  $\beta$ -C<sub>12</sub>G<sub>2</sub>, C<sub>12</sub>TAB, SDS and AOS to different gases.

The common feature of all foam films is that their permeabilities to different gases are different. It appears, from Figure 6, Figure 7 and Table 3, that gas permeability of foam films stabilized by different types of surfactants increases with increasing gas solubility in the liquid layer and most probably in the hydrocarbon phase present in the monolayer. Note that solubility of gas in pure water (i.e. central layer of the film) or pure hydrocarbon (i.e. hydrocarbon part of the surfactant molecules adsorbed at the film surface) may differ from its solubility in the liquid inside the film. The difference between permeabilities of Air and Xe is also noticeable and of particular importance. Since Xe has a high molecular weight and thus visible with CT scanner, Nguyen et al (2009) used it as tracer gas to determine the trapped fraction of foam.

In a simplistic view one might think that gas permeability varies linearly with inverse of viscosity of the gases. Table 3 summarizes the permeability of foam films stabilized by hexadecyltrimethylammonium bromide (C<sub>16</sub>TAB) in the presence of NaBr to number of gases. The permeability values are taken from Princen and Mason (1965). We have added viscosity of the gases and updated Henry's-law constants for the gases (Sander, 1999). Figure 8 shows the plot of permeability of foam film as a function of product of diffusion coefficient in water and Henry's-law constant (D×H) of the gases. The plot implies that the greater the product of diffusion coefficient in water and Henry's-law constant (D×H), the higher the permeation rate is (except for Helium). The correlation with inverse of viscosity fails, especially when gas solubility is high.

**Table 3:** Gas permeability of NBFs stabilized with C<sub>16</sub>TAB+0.1% NaBr to different gases

Gas	K (cm/s) <sup>§</sup>	H* (-)	μ (μP) <sup>#</sup>	D (10 <sup>-5</sup> cm <sup>2</sup> /s) <sup>&amp;</sup>	D*H (10 <sup>-5</sup> cm <sup>2</sup> /s)
N <sub>2</sub>	0.131	0.0132	178.1	2.0	0.026
Ne	0.211	0.0110	311.1	2.8	0.031
O <sub>2</sub>	0.321	0.0318	201.8	2.3	0.073
Ar	0.322	0.0342	221.7	2.3	0.079
He	0.398	0.0093	190.0	6.8	0.063
H <sub>2</sub>	0.577	0.0191	87.6	5.0	0.095
N <sub>2</sub> O	4.31	0.6112	148.8	1.8	1.131
CO <sub>2</sub>	7.85	0.8313	148.0	1.9	1.579

<sup>§</sup> Data taken from: Princen and Mason, 1965.

\* Data taken from: Sander, 1999.

<sup>#</sup> Data taken from: CRC handbook of chemistry and physics, 1980.

<sup>&</sup> Data taken from: Wise and Houghton, 1966.

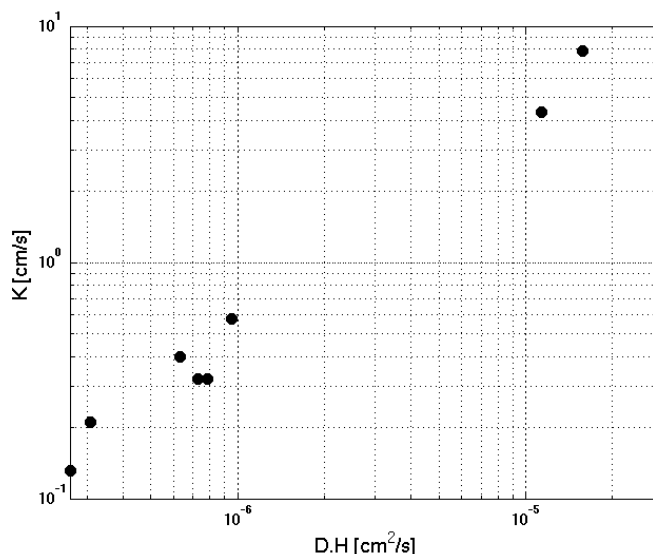


**Figure 8:** Gas permeability vs. product of Henry's-law constant and diffusion coefficient of the gases in Table 3.

Eq. (3) should apply to the initial composition of the bubble. To check the validity of Eq. (3) for mixture of gases over time, we calculated the permeability of foam films to air using the measured values of nitrogen and oxygen alone. Table 4 compares the measured and calculated values of permeability of the films to air. In the calculation we assumed that air consists of 78% N<sub>2</sub>, 21% O<sub>2</sub>, and 1% Ar. The agreement between the two values is good. The value of  $K$  for air reflect an average over the period when the gas bubble shrinks from about 100 or 150 μm in diameter to about 20 μm, and the bubble becomes more concentrated in N<sub>2</sub>. This average is not too far off from the value predicted by Eq. (3), that should apply at the start of the experiment with the initial gas mixture. As expected, the time-average value of  $K$  for this period is closer to the value for N<sub>2</sub> than one would expect for the initial composition of the bubble.

We obtained negative values for permeability of films stabilized by β-C<sub>12</sub>G<sub>2</sub> to oxygen and argon. It is possible that either the space above the surfactant solution or the solution itself was not completely saturated with the gases. However, since oxygen and argon have a similar solubility in water we can assume that the permeability of films stabilized by β-C<sub>12</sub>G<sub>2</sub> to both gases are the same (as is true for C12TAB and SDS). Therefore, using Eq. (3) and the values obtained for air and nitrogen we can calculate the permeability of these films to oxygen. The results are presented in Table 5. Once again the gas permeability of thicker CBF is higher than thinner NBF.

**Table 4:** Comparison of measured and calculated (Eq. 3) values of permeability of foam films to Air.

Surfactant	NBF, measured	NBF, calculated	CBF, measured	CBF, calculated
SDS	0.0395	0.383	0.2040	0.172
C <sub>12</sub> TAB	0.2540	0.277	0.263	0.280
$\beta$ -C <sub>12</sub> G <sub>2</sub>	0.0088	-	0.0153	-

**Table 5:** Gas permeability of film stabilized by  $\beta$ -C<sub>12</sub>G<sub>2</sub> to Oxygen calculated from Eq. (3)

Film type	K (cm/s)
NBF	0.03 $\pm$ 0.01
CBF	0.06 $\pm$ 0.01

#### 4. Implications for measuring trapped gas in foam flow in porous media

If one estimates a tortuosity factor ( $SL/V$ )  $\sim$  0.1 in Eq. (4), then  $D_e \sim (KL/10)$ . Values of  $K$  in this study range from about 0.03 cm/s to 0.60 cm/s. If one estimates that the distance between lamellae in trapped foam  $L$  is about 150  $\mu$ m, then the effective diffusion coefficient of tracer through foam ranges from  $5 \times 10^{-5}$  cm<sup>2</sup>/s to about  $10^{-3}$  cm<sup>2</sup>/s for these gases and surfactants. For Xenon, the tracer used in the study of Nguyen et al. (2009), the value of  $K$  in Table 5 suggests  $D_e \sim 1.7 \times 10^{-4}$  cm<sup>2</sup>/s, albeit with a different surfactant than used by Nguyen et al. (AOS and SDS are both anionic surfactants and their permeabilities to air are comparable (Fig. 5), so the value for Xe may be similar as well.) This value is close to that used by Kil et al. (2009) in estimating flowing-gas fraction from the CT images of Nguyen et al. It is smaller than the value estimated by Nguyen et al.,  $2 \times 10^{-3}$  cm<sup>2</sup>/s, based on apparent diffusion of tracer from the endplate of the apparatus, and the value of  $10^{-3}$  cm<sup>2</sup>/s used by Li et al. (2007) to fit the same experiment to a 3D model of convection and mass transfer.

For given bubble size, a relatively small effective diffusion coefficient through the trapped foam is best (Kil et al., 2009). All of the gases examined here permeate foam films faster than nitrogen, the main component of foam in the tracer studies. The next best among those examined here appears to be Neon (Table 3), for which one would estimate  $D_e \sim 3 \times 10^{-4}$  cm<sup>2</sup>/s. As shown by Kil et al. (2009), this implies diffusion fast enough to cause very rapid interaction of flowing and trapped gas, and render the usual method of interpretation of tracer data with a capacitance model inaccurate.

The estimated effective diffusion coefficient of CO<sub>2</sub>, used as a tracer by Tang and Kovscek (2006), is 60 times that of nitrogen (Table 3). In this case one would expect CO<sub>2</sub> to diffuse into trapped gas long before nitrogen diffuses back, causing swelling of the trapped gas and eventually intrusion of the trapped gas bubbles into the paths of flowing gas as discussed in Section 1.2. The large permeability coefficient of foam films to CO<sub>2</sub> has been suggested to be one the reasons for the differences observed between the stability of (sub-critical) CO<sub>2</sub> and N<sub>2</sub> foams in coreflood experiments (Farajzadeh et al., 2009b).

If one employed a tracer absolutely zero permeability through foam films, nitrogen would still diffuse out of trapped gas into the flowing gas with a lower partial pressure of nitrogen, causing shrinkage of trapped gas as described in Section 1.2. To avoid shifts in volume of trapped gas, the best tracer would be one used at the lowest measurable concentration, with close to the permeability of the gas in the foam; this puts a lower limit on the effective diffusion coefficient for tracer in an experiment. The permeability of nitrogen in Table 3 implies an effective diffusion coefficient through trapped foam of order  $2 \times 10^{-4}$  cm<sup>2</sup>/s, the value used by Kil et al. to analyze the Xenon tracer experiment. This was sufficient for substantial mass transfer between flowing and trapped gas, and introduced substantial errors into the interpretation of the tracer experiment using the conventional capacitance model in that study.

#### 5. Conclusions

- The permeability of foam films stabilized by three types of surfactants (anionic, cationic, and non-ionic) to different gases with different solubility in water was experimentally determined. The measurements were done with two different electrolyte concentrations, one corresponding to common black films (with thickness of 10-15 nm) and the other to the thinnest Newton black film (with thickness of 5 nm).
- For anionic surfactant, the gas permeability of thicker films is less than that of thinner films. At equilibrium the permeability of foam films is governed by interplay between film surfaces and adsorption of surfactants and not simply the thickness of the liquid layer.
- The permeability of foam films stabilized by all types of surfactants differs for different gases.

- There is a relationship between the solubility and diffusion coefficient of the gas in water and its permeation rate through a foam film. The film permeability is higher when solubility and diffusion coefficient of the gas in water are greater.
- The film permeability values measured here are consistent with the effective diffusion coefficient assumed by Kil et al. in their interpretation of foam tracer experiments. This magnitude is sufficient to make interpretation of foam tracer experiments using the conventional capacitance model difficult.
- If the film permeability of tracer is much larger than that of the gas in the foam, one would expect tracer to swell the trapped gas in the foam before the remaining gas has a chance to diffuse out. If the tracer has much smaller film permeability than the other gas, the trapped gas may shrink from diffusion of gas out. In either case, interpretation of the experiment is rendered more difficult.
- To avoid complications in the interpretation of results, the best tracer would be one with a permeability close to the permeability of the gas in the foam. This puts a lower limit on the effective diffusion coefficient for tracer in an experiment.

## 6. Acknowledgement

The first author of this paper thanks Shell International E&P for granting permission to complete and publish this work. T. Matsuura and M. Buijse are also acknowledged for careful review of the manuscript.

## 7. References

- Alvarez, J. M., Rivas, H., and Rossen, W.R., *SPE J*, 6 (2001) 325-333.
- Barnes, G. T., *Adv. Coll. Int. Sci.*, 25 (1986) 89.
- Barnes, G. T., D. Kashchiev, D. Exerowa, *Biophys. Biochem. Acta*, 732 (1983) 133.
- Binks, B. P. and T.S. Horozov, *Angew. Chem.*, 117, (2005) 3788–3791.
- Bird, R. B., Stewart, W. E., and Lightfoot, E. N., *Transport Phenomena* (2<sup>nd</sup> ed.), Wiley, 2002.
- Brown, A. G., W. C. Thuman and J. W. McBain, *J. Colloid Sci.*, 8, 508 (1953).
- Cohen, D., T.W. Patzek, C.J. Radke, *J. Colloid Interf. Sci.*, 179, 357-373 (1996).
- Cohen, D., T.W. Patzek, C.J. Radke, *Transport in Porous Media*, 28, 253-284 (1997).
- CRC handbook of chemistry and physics, editors, A. C. Weast and M.J. Astle, CRC Press INC., 1980, 60<sup>th</sup> Edition.
- Deryaguin, B.V., L.D. Landau, *Acta Phys. Chim. USSR* 14 (1941) 633; E.J.W. Verwey, J.T.G. Overbeek, *Theory of the Stability of Lyophobic Colloids*, Elsevier, Amsterdam, 1948.
- Dimitrov, D. *Compt Rend Akad Bulg Sci* 1977, 30, 269.
- Exerowa, D. and P.M. Kruglyakov, *Foam and Foam Films*, Elsevier Science, 1998.
- Falls, A. H., Lawson, J. B., and Hirasaki, G. J., *J Petr. Technol.* 40, 95-104 (1988).
- Farajzadeh, R., R. Krastev, P.L.J. Zitha, *Advances in Colloid and Interface Science*, 137(1), 27-44 (2008a).
- Farajzadeh, R., R. Krastev, P.L.J. Zitha, *Colloids and Surfaces A: Physicochem. Eng. Aspects*, 324 (2008b) 35–40.
- Farajzadeh, R., R. Krastev, P.L.J. Zitha, *Langmuir* (2009a) 25, 2881-2886.
- Farajzadeh, R., A. Andrianov, J. Bruining., P.L.J. Zitha, *Ind. Eng. Che. Res.*, 48 (2009b) 4542-4552. (also SPE 122133).
- Fried, A. N., *The foam-drive process for increasing the recovery of oil*, US department of Interior, Bureau of Mines (1961).
- Hanwight, J., J. Zhou, G. M. Evans, K. P. Galvin, *Langmuir*, 21 (2005) 4912-4920
- Israelachvili, J. and H. Wennerstrom, *J Phys Chem*, 96 (1992) 520.
- Janssen, L. P. B. M., and Warmoeskerken, M. M. C. G, *Transport Phenomena Data Companion*, VSSD, Delft, The Netherlands, 3rd ed., 2006.
- Kil, R. A., Nguyen, Q. P., and Rossen, W. R.: "Determining Trapped Gas in Foam From CT Images," SPE 124517 presented at the 2009 SPE Annual Technical Conference and Exhibition, New Orleans, LA, 4–7 October 2009.
- Kovscek, A.R. and C.J. Radke, *Fundamentals of foam transport in porous media*, In: *Foams: Fundamentals and applications in the Petroleum Industry*, ACS Advances in Chemistry Series, N.242, American Society (1994).
- Krustev, R., D. Platikanov and M. Nedyalkov, *Colloids and Surfaces A: Physicochem. Eng. Aspects*, 79 (1993) 129.
- Krustev, R., D. Platikanov, M. Nedyalkov, *Langmuir* 12 (1996) 1688.
- Krustev, R. and H.-J. Müller, *Langmuir*, 15 (1999) 2134.
- Krustev, R. and H. –J. Müller, *Review of Scientific Instruments*, 73 (2002) 398.
- Krustev, R. and H. –J. Müller, *Review of Scientific Instruments*, 73 (2002) 398.

- Li, Z., Nguyen, Q. P., and Rossen, W. R., "3D Modeling of Tracer Experiments to Determine Gas Trapping in Foam in Porous Media," SPE 107287 presented at the European Formation Damage Conference, Scheveningen, The Netherlands, 30 May–1 June 2007.
- Li, Z., Nguyen, Q. P., and Rossen, W. R., subm. to *Energy and Fuels* (2010).
- Muruganathan, R. M., R. Krustev, H.-J. Müller, H. Mohwald, *Langmuir*, 20 (2004) 6352-6358
- Muruganathan, R. M., R. Krustev, H.-J. Müller, H. Mohwald, *Langmuir*, 22 (2006) 7981-7985.
- Nedyalkov, M.; Krustev, R.; Kashchiev, D.; Platikanov, D.; Exerowa, D., *Coll. Polym. Sci.*, 266 (1988) 291.
- Nedyalkov, M.; Krustev, R.; Stankova, A.; Platikanov, D. *Langmuir*, 8 (1992) 3142.
- Nguyen, Q. P., Rossen, W. R., Zitha, P. L. J., and Currie, P. K., *SPE J*, 14 (2009) 222-236.
- Platikanov D, M Nedyalkov, V. Nasteva, *J Coll Interf Sci*, 75 (1980) 620.
- Princen, H. M. and S. G. Mason, *J. Colloid Sci*, 20 (1965) 353.
- Princen, H. M., Th. G. Overbeek, S. G. Mason, *J. Colloid Sci*, 24 (1967) 125-130.
- Radke, C.J. and Gillis, J.V.: "A Dual Tracer Technique for Determining Trapped Gas Saturation during Steady Foam Flow in Porous Media," paper SPE 20519 presented at the 65th Annual Technical Conference and Exhibition, New Orleans, 1990.
- Rossen, W. R. In: R. K. Prud'homme and S.A. Khan, Editors: *Foams, theory, measurements and application*, New York, Marcel Dekker, Inc., 1996, p.413-463.
- Sander, R. Compilation of Henry's-Law Constants for Inorganic and Organic Species of Potential Importance in Environmental Chemistry, available online at: <http://www.mpch-mainz.mpg.de/%7Esander/res/henry.html>, Version 3, 1999, p57 (last date accessed Feb. 2010)
- Tang, G.-Q., and A. R. Kovscek. *Transport in Porous Media*, 65 (2006) 287-307.
- Wise, D.L. and G. Houghton, *Chem. Eng. Sci.* 21 (1966) 999-1010.